Journal Pre-proofs

Drug-eluting wound dressings having sustained release of antimicrobial compounds

Enrique Gámez-Herrera, Sara García-Salinas, Sofía Salido, María Sancho-Albero, Vanesa Andreu, Marta Pérez, Lluís Luján, Silvia Irusta, Manuel Arruebo, Gracia Mendoza

PII: S0939-6411(20)30152-1
DOI: https://doi.org/10.1016/j.ejpb.2020.05.025
Reference: EJPB 13315

To appear in: *European Journal of Pharmaceutics and Biopharmaceutics*

Received Date: 27 November 2019
Revised Date: 12 May 2020
Accepted Date: 25 May 2020

Please cite this article as: E. Gámez-Herrera, S. García-Salinas, S. Salido, M. Sancho-Albero, V. Andreu, M. Pérez, L. Luján, S. Irusta, M. Arruebo, G. Mendoza, Drug-eluting wound dressings having sustained release of antimicrobial compounds, *European Journal of Pharmaceutics and Biopharmaceutics* (2020), doi: https://doi.org/10.1016/j.ejpb.2020.05.025

Drug-eluting wound dressings having sustained release of antimicrobial compounds

Enrique Gámez-Herrera[a], Sara García-Salinas[a,b], Sofía Salido[c,] María Sancho-Albero[a,b,d], Vanesa Andreu[a,d], Marta Pérez[e], Lluís Luján[e], Silvia Irusta[a,b,d,*], Manuel Arruebo[a,b,d,*], Gracia Mendoza[a,b,d]

[a]Department of Chemical Engineering. Aragon Institute of Nanoscience (INA), University of Zaragoza, Campus Río Ebro-Edificio I+D, C/ Poeta Mariano Esquillor S/N, 50018 Zaragoza, Spain

[b]Networking Research Center on Bioengineering, Biomaterials and Nanomedicine, CIBER-BBN, 28029 Madrid, Spain

[c]Department of Inorganic and Organic Chemistry, Faculty of Experimental Sciences, University of Jaén, Agrifood Campus of International Excellence (ceiA3), 23071 Jaén, Spain

[d]Aragon Health Research Institute (IIS Aragon), 50009 Zaragoza, Spain

[e]Department of Animal Pathology, Veterinary Faculty, University of Zaragoza & AgriFood Institute of Aragon (IA2), C/ Miguel Servet, 177, 50013 Zaragoza, Spain

Corresponding authors: *Email addresses: sirusta@unizar.es (S.I.), arruebom@unizar.es (M.A.). Department of Chemical Engineering, Aragon Institute of Nanoscience (INA), University of Zaragoza, Campus Río Ebro-Edificio I+D, C/ Mariano Esquillor S/N, 50018 Zaragoza, Spain

ABSTRACT

Wound healing is a complex and costly public health problem that should be timely addressed to achieve a rapid and adequate tissue repair avoiding or even eliminating potential pathogenic infection. Chronic infected non-healing wounds represent a serious concern for health care systems. Efficient wound dressings with tailored therapy having the best response and highest safety margin for the management of chronic non-healing wounds are still needed. The use of novel wound dressing materials has emerged as a promising tool to fulfil these requirements. In this work, asymmetric electrospun polycaprolactone (PCL)-based nanofibers (NFs) were decorated with electrosprayed poly(lactic-co-glycolic acid) microparticles (PLGA MPs) containing the natural antibacterial compound thymol (THY) in order to obtain drug eluting antimicrobial dressings having sustained release. The synthesized dressings successfully inhibited the *in vitro* growth of *Staphylococcus aureus* ATCC 25923, showing also at the same doses cytocompatibility on human dermal fibroblasts and keratinocyte cultures after treatment for 24h, which was not observed when using free thymol. An *in vivo* murine excisional wound splinting model, followed by the experimental infection of the wounds with *S. aureus* and their treatment with the synthesized dressings, pointed to the reduction of the bacterial load in wounds after 7 days, though the total elimination of the infection was not reached. The findings indicated the relevance of the direct contact between the dressings and the bacteria, highlighting the need to tune their design considering the wound surface and the nature of the antimicrobial cargo contained.

Keywords: wound infection, dressing, electrospinning, antibacterial nanomaterials, thymol, *in vivo* murine model, non-healing wounds.

1. Introduction

Acute wounds including surgical wounds, burns, pressure and diabetic foot ulcers, fistulas, edemas, etc. may suffer from potential bacterial infection and subsequent impaired healing and even possible chronification. Bacterial colonization can be originated by the host microbiota present on the skin or in other parts of the body or by environmental exposure to pathogenic microorganisms. Infected wounds are treated by debridement (i.e., removal of devitalized tissue), cleansing, drainage and, depending on the wound culture results, systemic or topical antibiotic treatment. Different reports have quantified the direct and indirect costs associated to chronic non-healing infected wounds and all of them alert about population aging and comorbid growing illnesses, such as diabetes, as concerns which might increase even further the tremendous social and health care burden that they represent [1,2].

After wounding, dressings are primary used to protect the new forming tissue from external physical and biological contamination, to control the drainage of excess fluid and potential bleeding and to allow adequate vapor permeability to avoid maceration. Drug-eluting wound dressings are used to locally release a drug, antibiotic or antiseptic to remove pathogenic bacteria and accelerate the natural healing process while preventing the bacteria from leaking out and spreading. Some of the commercially available ones include silver and gentamicin in their formulation to take advantage of the wide antimicrobial spectrum of the former and the antibiotic activity of the later against a wide range of bacterial strains, mostly Gram-negative bacteria [3]. One of the limitations to overcome of topic antibiotics and antiseptics is the potential cytotoxicity against eukaryotic cells of the released antimicrobial, as well as the potential development of bacterial antibiotic resistance. Also, a

prolonged antimicrobial release from the dressing is sought considering that during the healing process potential bacterial contamination might occur at any time. Molecular genetics have determined the existence of silver resistance thanks to the identification of the responsible bacterial plasmids and genes [4]. Likewise, gentamicin resistance was initially reported early in 1970 soon after its discovery (1963) [5]. In addition, topical antibiotics avoid systemic side effects, provide with a localized targeted effect on the wound bed and allow the use of some antibiotics that are disapproved for systemic administration. However, cytotoxicity on human cells due to the high site concentration remains as the main limitation of topical antibiotics as well as the aforementioned potential development of antibiotic resistance. Gentamicin, for instance, presents as adverse side effects ototoxicity and nephrotoxicity as well as keratinocyte inhibition when used topically at high doses [6]. Gentamicin loaded electrospun wound dressings have previously shown at short times higher cytotoxicity against human fibroblasts than controls and a delayed healing process [7]. Silver is cytotoxic against keratinocytes and fibroblasts and may inhibit re-epithelialization when extensively applied on the infected wound bed [8]. Therefore, antimicrobial resistance and toxicity against eukaryotic cells remain as drawbacks needed to be addressed. Several other wound dressings have been developed to reduce the antibiotic cytotoxicity on human cells by fine-tuning its release kinetics while having large antibacterial action [9–12]; however, in those pads, antibiotic resistance remains still as a foremost threat. In addition, there is limited evidence for differences between wound dressings for any outcome in some non-healing chronic wounds such as foot ulcers in people with diabetes [13]. Therefore, efficient wound dressings with tailored therapy having the best response and highest safety margin for the management of chronic non-healing wounds are still needed.

After analyzing 1770 wounds, Twum-Danso et al. identified *Staphylococcus aureus* 23.7%, *Escherichia coli* 16.9%, *Staphylococcus epidermidis* 13.5% and *Pseudomonas aeruginosa* 13.0% as the most common pathogens identified in intra-operative wounds whereas *Enterobacter spp.*, *Proteus spp.*, *Klebsiella spp.* and *P. aeruginosa* had a higher presence on postoperative wounds [14]. The microbiological analysis of chronic infected wounds such as diabetic foot ulcers from 313 tissue samples obtained from 222 patients previously treated with antibiotics identified *Pseudomonas aeruginosa* and *Acinetobacter spp.* as the most common pathogens in both bone and soft tissues [15]. However, the identification of specific bacteria in a wound does not necessary mean that the wound is infected. Genotyping by DNA sequencing aids in identifying the complete combined microbiome in infected wounds. However, the identification of planktonic bacteria is not an easy task because its growth is a dynamic process that changes over time, depends on the sampling methods used and the bacteria is not homogeneously distributed along the wound and also it is not only present on the external surface but also it can be present deeply in the tissue. Another additional limitation is that molecular assays such as 16S rRNA PCR and the ones based on partial ribosomal amplification are able to identify bacteria including viable but nonculturable (VBNC) bacteria but genetic material coming from non-viable bacteria is also accounted when using those analytical techniques [16].

The complexity of identifying the microbiome present in infected wounds is a handicap and also the already mentioned antibiotic resistance but, in addition, the presence of bacterial biofilm associated to non-healing chronic (> 1 month) infected wounds represents a major limitation that constitutes a serious concern. The identification of bacterial biofilm on infected wounds is not a straightforward task and a compendium between morphological

and microscopic analysis, conventional microbiological techniques and molecular assays including transcriptomics and wound blotting are recommended to confirm its presence [16]. In 2017, a Global Wound Biofilm Expert Panel delivered a consensus document settling the guidelines for the identification and treatment of biofilms in chronic non-healing wounds [17]. Two key guidelines with which all the experts strongly agree were that: 1) Repeated debridement alone fails in preventing biofilm regrowth and the use of topical antiseptics up to 24h after debridement reduces the chances of forming biofilm within this time-dependent window and 2) A sustained active level of antimicrobial at a concentration above the Minimum Biofilm Eradication Concentration (MBEC) is required to prevent biofilm formation. Therefore, a sustained antimicrobial release should be provided within this time-dependent window after debridement and novel drug-eluting dressings with sustained antimicrobial release are demanded.

Herein, we have developed drug eluting antimicrobial dressings with time-controlled drug release and with the ability to release natural-origin antiseptics. Asymmetric electrospun dressings were obtained by decorating polycaprolactone (PCL) nanofibers (NFs) with electrosprayed poly(lactic-co-glycolic acid) microparticles (PLGA MPs) containing the natural antimicrobial cargo. As we mentioned before, a prolonged antimicrobial release from the dressing is sought considering that during the healing process potential bacterial contamination might occur at any time. Those natural compounds have multiple mechanisms of antimicrobial action and the chances for the bacteria of acquiring simultaneous genetic mutations are reduced compared to the use of antibiotics, which usually have a single target. THY was the natural monoterpenoid phenol chosen due to its well-known antimicrobial [18–20] and anti-inflammatory [21] action. It is well known that

proinflammatory cytokines are overexpressed in chronic wounds [16] therefore; healing can be promoted by the sustained release of compounds with both antiseptic and anti-inflammatory effects. In this work, at the same doses, non cytotoxicological effects were observed on eukaryotic cells whereas antimicrobial action was observed, and a sustained release was responsible of an increased antimicrobial action over time. We previously fabricated electrospun PCL-based THY-loaded nanofibers [22] and tested their antimicrobial efficacy *in vitro*. However, in that preliminary study only the THY present on the external surface of the nanofibers was released (~7% of the thymol loaded) and the rest of the thymol incorporated (~93%) remained in the interior of the fibers due to the slow degradative rate of PCL. Herein, we have included THY within PLGA-based microparticles decorating the nanofibers in order to achieve a sustained release of the antimicrobial compound for a long time. We took advantage of the hydrolytic character of the ester bonds present in PLGA to release large amounts of the encapsulated antibacterial compound in a sustained manner providing with a pharmacokinetic control of the release.

2. Materials and methods

2.1. Materials

PCL (*Mn* = 80000 Da), (*S*)-(-)-limonene (food grade ≥ 95 %), naproxen sodium salt (98-102 %), piperonal (3,4-(methylenedioxy)benzaldehyde, 99.8%), phosphate buffer saline (PBS) and Tween 80 were purchased from Sigma-Aldrich. Dichloromethane (DCM > 99 %) and *N*,*N*-dimethylformamide (DMF > 99 %) were obtained from Fisher Scientific. PLGA RESOMER RG 504 was purchased from Evonik Industries AG. Thymol (99 %) was purchased from Acros Organics. Trypticase in soy broth (TSB) and trypticase in soy agar (TSA) were obtained from Laboratorios Conda-Pronadisa S.A. Deuterated chloroform

(99.8 % D), acetonitrile (≥ 99.9 %), methanol (≥ 99.9 %) and formic acid (98-100 %) were purchased from VWR. Dulbecco's Modified Eagle's Medium (DMEM) containing L-glutamine (2 mM) and antibiotics (1 % penicillin-streptomycin-amphotericin B) was obtained from Biowest. Fetal Bovine Serum (FBS, 10 % v/v) was used for supplement DMEM and purchased from Gibco. All reagents were used without any further purification.

2.2. Fabrication of PCL electrospun mats decorated with electrosprayed thymol-loaded PLGA microparticles

Initially, nanofibrous mats were prepared by electrospinning in an Yflow 2.2 D500 electrospinner equipped with an 8 cm aluminium disc covered with an aluminium foil as collector. A solution of PCL (10 % w/w) was prepared by overnight stirring it at room temperature in a mixture of DCM and DMF (1:1 v/v). A 10 mL syringe was filled with the polymeric solution that was sonicated for 15 min to remove occluded air bubbles before connecting it with the electrospinner.

A 2D module (to allow the dual axis movement of the needle) was used in order to obtain mats with homogenous thicknesses. A 22-gauge needle was used and the distance needle-collector was fixed at 18 cm with a flow rate fixed at 1.0 mL/h. The voltage applied to the collector was -4.00 kV and the voltage applied to needle was +10.50 kV. All samples were obtained at room temperature with a relative humidity between 30 and 50 %.

After synthesis, empty or THY-loaded MPs were electrosprayed on one side of the electrospun mat surface in order to obtain mats decorated with electrosprayed THY-loaded PLGA MPs or free of THY as controls. With this purpose, a solution of PLGA (10 % w/w) in DMF containing different amounts of THY (0, 2.5, 5, 7.5, 10 and 15 wt. % referred to

the PLGA mass) was loaded in 10 mL syringes that were subsequently degassed by sonication for 15 min to remove potentially occluded air bubbles. Different amounts of THY were loaded within the electrosprayed PLGA microparticles in order to control the total amount of THY incorporated in the dressings. In our previous studies we evaluated the minimum inhibitory concentration (MIC) and minimum bactericidal concentration (MBC) for free THY against planktonic bacteria [19] and when incorporated within electrospun PCL nanofibers [22] highlighting the importance of the direct contact between bacteria and the antimicrobial mat to elicit antibacterial effects.

The same Yflow 2.2 D500 electrospinner and collector were employed to spray the thymol-loaded microparticles on the separately prepared mats. A 22-gauge needle was located at 30 cm from the collector plate where the previously prepared mat was placed. Flow rate was set at 0.5 or 1.0 mL/h. The voltage applied to collector was -4.30 kV and the voltage applied to the needle varied from +10.08 to +14.10 kV in order to obtain a stable Taylor cone jet. All samples were obtained at room temperature and a relative humidity between 30 % and 50 %. Hence, the MPs with THY (or without it as controls) were electrosprayed on one side of the previously prepared PCL electrospun mats.

2.3. Characterization of the hybrid mats

Scanning electron microscopy (SEM) was used for the morphological characterization of the materials prepared. Each sample was covered with a 5 nm Pd layer before the visualization in an Inspect F-50 SEM microscope. PLGA MPs and NFs diameters and standard deviations were measured using the ImageJ software (N = 100).

For the mechanical characterization of the fabricated mats, six samples per mat were cut into 50 mm × 10 mm pieces and subjected to a tensile test. Mechanical properties were determined using a uniaxial Instron test machine (Instron, US) with video extensometer 5548 (1 KN load cell, 1 mm/min).

Thymol concentration in the microparticles was determined by GC-MS. A calibration curve for THY was prepared from 1 to 50 ppm with 5 ppm of *S*-(-)-limonene as internal standard. Un-supported thymol-loaded microparticles (10 mg) were dissolved in 10 mL of acetonitrile. 500 µL of solution (with an adequate concentration of internal standard) was mixed with 500 µL of methanol, centrifuged for 15 min at 13300 rpm and supernatant was filtered (200 nm cut off) in order to remove precipitated PLGA. Supernatant was diluted with methanol (to fit the sample concentration to the calibration curve) and analysed in a Shimadzu 2010SE GC-MS chromatograph with an AOC 20i injector. A Zebron ZB-50 capillary column (30 m x 0.25 mm, 0.25 µm thickness, Phenomenex) was used. The chromatographic method included a heating increase from room temperature to 50 °C with a dwell time of 1 min then an increase at 160 °C at 10 °C/min and a final rise to 200 °C at 20 °C/min. Helium, at a constant flow rate of 1.0 mL/min, was used as carrier gas. The detector temperature was 250 °C and the transfer line and ion source temperature were both set at 200 °C. For analysis, 1 µL of sample was injected, working with a split ratio of 1:10. Data were obtained from three independent experiments run in duplicate.

Also, a quantitative ^{1}H NMR (qNMR) method has been used to confirm the percentage of PLGA ester and THY loaded in the hybrid mats.^{1}H NMR spectra were recorded at 400 MHz on a NMR spectrometer (Bruker DPX 400, Bruker Daltonik GmbH) over a spectral width of 0-13 parts per million (ppm) and chemicals shift values (δ) were reported in ppm.

To obtain the maximum signal intensity of each proton in quantitative NMR spectra, an optimization of relaxation delay parameter, D_1, has been performed. For that, the inversion recovery-pulse sequence was used to calculate spin-lattice relaxation, T_1, in PCL, PLGA ester, THY and internal standard (piperonal) solutions, while the 90° pulse width was 10.4μs. The highest value at T_1 was 4.45 s, corresponding to the piperonal signal with chemical shift at 9.80 ppm. Therefore, the D_1 parameter was fixed at 15 s (more than 3 times the T_1 value). Other values for the acquisition parameters of the ^{1}H NMR spectra were as follows: acquisition time (1s); number of scans (16); temperature (27.0 °C).

For sample measure, piperonal was used as internal standard and five calibration solutions were prepared. Solutions were prepared in 5 mm OD NMR tube from four standard solutions in $CDCl_3$ of PCL (4 mg/mL), PLGA (4 mg/mL), thymol (4 mg/mL) and piperonal (5 mg/mL). The amount of piperonal was the same for samples and calibration curves. The signal selected from ^{1}H NMR spectra to assign the integral value of 1 was the singlet signal of piperonal at 9.80 ppm. For quantification of thymol, PLGA ester and PCL, the doublet signal at 7.05 ppm of THY, the multiplet signal at 4.53-4.95 ppm of PLGA ester and the multiplet signal at 3.95-4.10 ppm of PCL were chosen. Lineal regression plots were obtained in order to calculate the mass of PLGA ester per mass of internal standard and the mass of THY per mass of internal standard. Data were obtained from three independent experiments run in duplicate.

2.4. In vitro release kinetics of PCL-electrospun mats decorated with thymol-loaded microparticles

25 mg of the PCL-electrospun mats decorated with THY-loaded microparticles were immersed in 10 mL of PBS (with Tween 80, 2 % w/v). Samples were kept at 37 °C with a

constant agitation (250 rpm). PBS was replaced at different time (each 0.5 h from 0 to 3h, each hour from 3 to 8 h, 24, 72, 120, 192 and 360h). Collected samples were analysed by UPLC with an Acquity UPLC® Waters liquid chromatographic system equipped with a column heater, a photodiode array detector ACQ-PDA, a quaternary solvent manager ACQ-QSM and a sample manager ACQ-FTN controlled by Waters® Empower™ chromatographic software. An Acquity UPLC® Waters BEH C18 column (2.1 x 50 mm, 1.7 µm particle diameter) protected by 0.2 µm stainless steel In-Line Filter with a Holder Waters was used.

A calibration curve from 2.5 to 300 ppm was prepared for the THY analysis. 25 ppm of naproxen sodium salt was added to the samples as internal standard. For the analysis, an isocratic method at 40 °C was employed. Mobile phase was composed by a mixture of acetonitrile and milli-Q water (with formic acid, 0.1 % v/v) in a proportion 50:50 in volume. THY was detected and quantified using the PDA detector set at 275 nm wavelength. THY released concentrations were obtained from three independent experiments run in duplicate and analysed in triplicate by UPLC.

To evaluate the release kinetics, data fitted the Peppas-Sahlin model. The correlation coefficient (R^2) value was calculated from the linear regression of these plots by means of the following equation (Eq. 1):

Peppas-Sahlin model: $$\frac{M_t}{M_T} = k_1 t^n + k_2 t^{2n} \qquad \text{[Eq. 1]}$$

where M_t/M_T is the drug release fraction at time t; k_1 and k_2 are constants from Fickian diffusional contribution and case-II relaxation contribution, respectively; n is the diffusional exponent that can be related to the drug transport mechanism.

2.5. Antibacterial activity determination

Antibacterial activity of synthetized materials against *Staphylococcus aureus* ATCC 25923 (Ielab) was tested with the Antimicrobial Disk Susceptibility Tests of the US Clinical and Laboratory Standards Institute (CLSI) [23]. The PCL electrospun mats developed (PCL electrospun NFs, PCL electrospun NFs decorated with PLGA microparticles (PCL NFs@PLGA MPs), and PCL electrospun NFs decorated with electrosprayed thymol-loaded PLGA microparticles (PCL NFs@PLGA-THY MPs) were cut as discs of different diameters (12, 14, 18 and 20 mm), and sterilized under UV light (30 min on each side). The agar petri dishes were inoculated with 200 µL of a suspension of *S. aureus* (10^7 Colony Forming Units per mL, CFU/mL). Samples were placed in the inoculated petri dishes (2 samples/dish) with the side of thymol-loaded PLGA microparticles in contact with the agar in the case of PCL NFs@PLGA-THY MPs mats.

2.6. In vitro cytotoxicity study

Human dermal fibroblasts (Lonza) and keratinocytes (HaCaT; kindly donated by Dr Pilar Martín-Duque) were used to evaluate the possible cytotoxic effects of the electrospun mats developed in a potential topical application.

Both cell lines were cultured at 37 °C in a 5 % CO_2 atmosphere in DMEM containing L-glutamine (2 mM) and supplemented with FBS (10 % v/v) and antibiotics (1 % penicillin-streptomycin-amphotericin B). To assess the viability after treatment for 24h with free THY and with the electrospun materials developed, PCL NFs, PCL NFs@PLGA MPs and PCL NFs@PLGA-THY MPs, cells were seeded in 6-well plates (1.2 x 10^5 cells/well). After 24h to assure cell attachment, medium was discarded and replaced with fresh medium

and free THY or PCL NFs, or PCL NFs@PLGA MPs, or PCL NFs@PLGA-THY MPs mats were added. For the mats, 20 mm discs were cut and sterilized under UV light (1h for each side). For free THY, 0.52 mg/mL concentration was selected as represents the total amount of THY released in 24h from the 20 mm diameter PCL NFs@PLGA-THY MPs mats. After incubation for 24h, the Blue Cell viability assay (Abnova) was performed to study the viability related to cell metabolism. The mats were discarded, the medium replaced adding the reagent (10% v/v) and incubated for 4h (37 °C, 5 % CO_2). Then, the fluorescence was read (535/590 nm ex/em) in a Synergy HT microplate reader (Biotek). Viability was calculated by data interpolation considering control samples (un-treated) as 100 % viability. The data shown are obtained from six experiments run in duplicate (12 data per material tested).

2.7. Preclinical wound infection model

The research was carried out under Project License 51/14 approved by the Ethic Committee for Animal Experiments of the University of Zaragoza (Spain). Eight to ten-week-old male SKH1 hairless mice (Charles River Laboratories) were used for this study. Mice were fed *ad libitum* and maintained under specific pathogen-free conditions accordingly with the Spanish Policy for Animal Protection RD53/2013, which meets the European Union Directive 2010/63 on the protection of animals destined to scientific purposes.

To evaluate wound infection and closure in murine skin avoiding wound contraction, the murine excisional wound splinting model with some modifications was carried out [24], as shown in Fig. 6A. This model mimics the human wound closure process through granulation and reepithelization by suturing a splinting ring around the wound, avoiding the typical murine healing through skin contraction [25]. Previously to the surgery and every

317 day after surgery, mice were weighted to check the potential weight loss during the
318 procedure. Animals were anesthetized with 5 % isoflurane, and maintained with 1-2 %
319 isoflurane and an oxygen flow of 1 L/min. The skin surface was disinfected with 70 %
320 ethanol (v/v). Meloxicam (2.5 mg/kg body weight) was then administered via sub-
321 cutaneous injection for pain relief before surgery and every day until 48h after surgery.
322 Two 8-mm-diameter full-thickness wounds were made aseptically in the skin by using a
323 sterile biopsy punch (Eickemeyer Veterinary Equipment Ltd.) in the thoracic region at each
324 side of the median line. Then, two donut-shaped silicone wound splints (Grace Bio-Labs)
325 were fixed into place around the wounds with six interrupted polyamide sutures (Dafilon
326 4/0; Braun). After suturing, infected wounds were inoculated with *S. aureus* ATCC 25923
327 (10^7 colony forming units (CFU) in 25 µL of PBS) and maintained uncovered for 15 min to
328 allow the bacterial dispersion to penetrate in the wounded skin. It should be noted that a
329 preliminary study of bacteria loading (10^2-10^9 CFU in 25 µL of PBS) was performed to
330 determine the minimum bacteria concentration to achieve a durable infected wound
331 considering the immunocompetence of the treated mice. After infection induction, different
332 discs of 12-mm-diameter PCL NFs@PLGA MPs mats or PCL NFs@PLGA-THY MPs
333 mats were piled up and placed onto the wounds to achieve the inhibitory THY
334 concentration obtained in the *in vitro* assays described above. Then, in order to protect the
335 wounds and the dressings, and to ensure an adequate progress of wound infection, an
336 occlusive sterile adhesive plaster and a sterile bandage (Hartmann) were used to cover the
337 wounds and splints. Mice were examined daily regarding infection progression, weight loss
338 and pain.

Twenty-four mice were experimentally divided in four groups (N = 6): i) Control group (wounds not infected); ii) Infected group (wounds infected and not treated with drug-eluting dressings); iii) Infected group treated with PCL NFs@PLGA MPs mats; iv) Infected group treated with PCL NFs@PLGA-THY MPs mats. Each subgroup underwent the sacrifice of three mice at 3 days and 7 days after wound surgery and infection. At these time points, wound sizes were measured and photographed. All wounds were exposed from the third day after surgery and infection, as indicated in the clinical practice [26,27].

2.8. Microbiological evaluation of wounds

Infection levels of surgical wounds were quantified by using microbiological swabs with Amies media (Deltalab) after 3 and 7 days of the surgery and infection. Swabs were grown on blood agar and McConkey No. 3 media (Oxoid) and then incubated at 37 °C for 24h to semiquantify the *S. aureus* levels in the wounds. To carry out the identification of the microorganism, samples were reseeded and analyzed by a MALDI-TOF system (Bruker). Furthermore, at the same time points, swab samples were also analyzed by quantitative polymerase chain reaction (qPCR) to determine and quantify the presence of the experimental *S. aureus* ATCC 25923 strain in the wounds and the potential reduction of the bacteria levels in treated wounds. In brief, bacterial DNA was extracted from the samples with the DNeasy Blood & Tissue Kit (Qiagen) and then amplified by using the EXOone *Staphylococcus aureus* one MIX qPCR kit (Exopol) and a 7500 FAST Real Time PCR System (Applied Biosystems), following a pre-incubation step consisted in 1 cycle of 5 min at 95 °C whereas the amplification step comprised 42 cycles of 15 s at 95 °C and 1 min at 60 °C. Then, the plate was read. All microbiological data were obtained from three independent experiments run in triplicate.

2.9. Pathological studies

Animals were euthanized by CO_2 inhalation at day 3 or day 7 after surgery and infection. Wound tissue samples were collected by carefully removing bandages, plasters, electrospun dressings, sutures and splints, along with 3 - 5 mm surrounding skin tissue. The wound samples were fixed in 4% buffered paraformaldehyde (Alfa Aesar) and embedded in paraffin. Five-micron-thick tissue sections were obtained and stained with hematoxylin and eosin (HE) staining for histopathological evaluation.

The pathological evaluation of the wounds also included measuring of angiogenesis by CD31 (Rabbit Polyclonal CD31 (ab28364), Abcam) using the automated immunostaining platform Autostainer Link (Dako). Briefly, slides were deparaffinized in xylene and re-hydrated by means of an ethanol series until water. Prior to the primary antibody incubation, the antigen retrieval was developed by high pH buffer treatment (CC1m, Roche) and the endogenous peroxidase was blocked through addition of 3% H_2O_2. Slides were then incubated with the primary antibody (Rabbit Polyclonal CD31 1:50 for 60 min) to be followed by the corresponding visualization system conjugated with horseradish peroxidase (EnVision FLEX+, Dako). The immunohistochemical reaction was carried out with the chromogen 3, 30-diaminobenzidine tetrahydrochloride (DAB), whereas Carazzi's hematoxylin was used for nuclei staining. For microscopic evaluation, the slides were then dehydrated and permanent mounted.

2.10. Statistical analysis

All statistics were performed using GraphPad software. Data are reported as mean ± SD. To test for statistical significance, two-way analysis of variance (ANOVA) for multiple

comparisons by Dunnett's multiple comparisons test was employed. Significant differences were considered when $p \leq 0.05$.

3. Results

3.1. Characterization of asymmetric electrospun antimicrobial dressings

In order to obtain reproducible drug-release kinetics, microparticle homogeneity in the electrosprayed materials was sought. Therefore, different THY concentrations and different flow rates used in the PLGA electrospraying were evaluated (Fig. 1). Particle size distributions revealed 1 mL/h flow rate and 10 wt.% THY concentration as the experimental conditions that produced a homogeneous particle size distribution (0.728 ± 0.143 μm) on the electrospun mats. At the same flow rate (0.5 mL/h), increasing the THY concentration (5 - 15 wt. %) a narrower particle-size distribution was found at 10 wt. % (Fig. 1C). At the same THY concentration (10 wt. %), a narrower particle size distribution was obtained with the highest flow rate tested (1 mL/h). Those conditions (10 wt.% THY and 1 mL/h flow rate) were selected for the subsequent experiments.

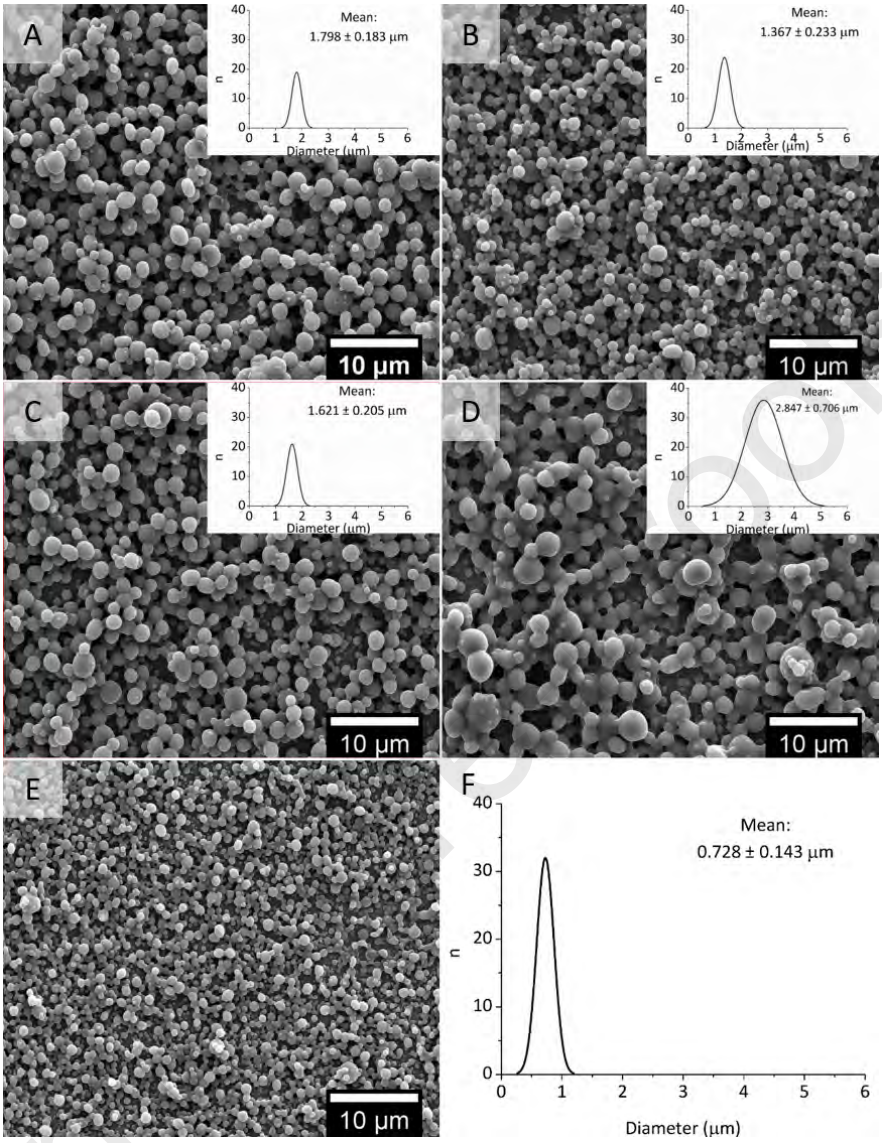

Fig. 1. Synthesis optimization for THY-loaded PLGA microparticles. A) 5 % THY, 0.5 mL/h; B) 7.5 % THY, 0.5 mL/h; C) 10 % THY, 0.5 mL/h; D) 15 % THY, 0.5 mL/h; E) 10 % THY, 1.0 mL/h; F) histogram of microparticles from image E (N = 100).

Figure 2 shows the increase in the microparticle loading on the electrospun NFs over time. The longer the electrospraying time, the higher the microparticle loading. Also PLGA MPs preferentially attached to the NFs and no loosely bound microparticles were found. The large area per volume ratio of the electrospun PCL mat provided with large surface area

available for electrostatic interaction. Microparticles were not present on the other side of the mat, therefore they did not percolate throughout the electrospun mat (Fig. 2F).

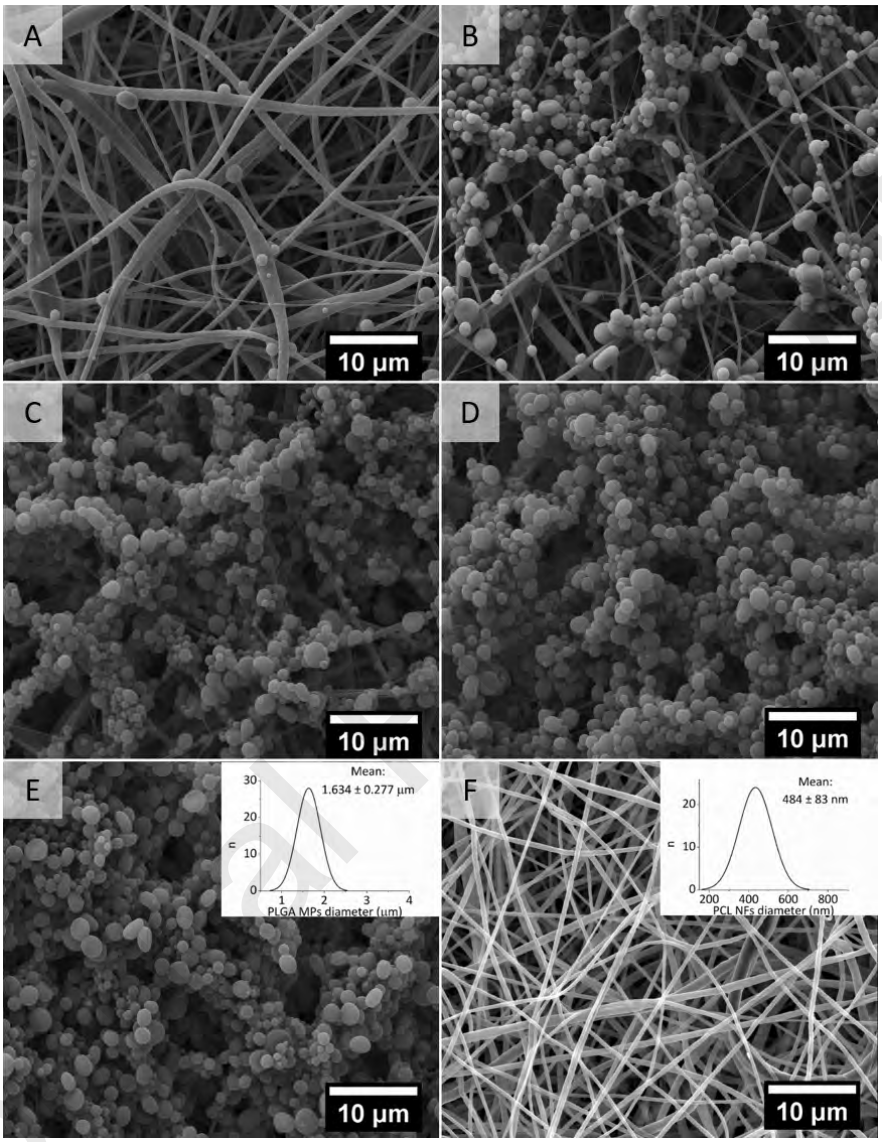

Fig. 2. Microparticle attachment on the electrospun PCL nanofibers over time: A-D) nanofibers surface after 0.5, 1, 1.5 and 2h of microparticle electrospraying, respectively; E) top-side view of electrospun PCL nanofibers after 2h of microparticle electrospraying; F) bottom-side of the mat after 2h of microparticle electrospraying. N = 100.

444 To test the strong attachment between the PLGA MPs and the electrospun NFs, mechanical
445 stress was evaluated by means of ultrasonic energy. The resulting mats were immersed in
446 water and subjected to 40 kHz at a constant power of 360 W up to 18 min at room
447 temperature. As is shown in Fig. 3 (A-D), the cavitation bubbles induced by the high
448 frequency sound waves did not detach the MPs from the electrospun PCL NFs. No PLGA
449 MPs were found on the bottom side of the mat indicating that the MPs were not able to
450 cross the 36 ± 8 μm-thick (evaluated by an analogic micrometer) mats due to their inherent
451 tortuosity. We assume that PLGA MPs could not percolate through the mats but as
452 observed the mats preserved porosity to allow vapor exchange.

453 The tensile strength (2.8 ± 0.2 MPa) and strain at break (174.0 ± 12.4%) values obtained for
454 the unloaded mats are in agreement with the previously reported values for PCL fibers
455 decorated with PLGA particles [28]. The incorporation of THY in the MPs slightly changed
456 these values, so the tensile strength measured was 2.7 ± 0.8 MPa whereas the strain at break
457 was 168.4 ± 0.4%. This fact was expected since the mechanical properties of the mats are
458 mainly given by PCL fibers that are not modified by THY incorporation. The tensile
459 strength was in the required range for wound dressing applications while the mats
460 elongation-at-break was around 140% higher than the value of the human skin [29].
461 The amount of PLGA and THY in the final mats was evaluated by means of NMR. As it is
462 shown in Fig. 3E, a PLGA content of 11.28 ± 3.39 and 17.46 ± 2.15 wt. % were obtained
463 for the PCL electrospun NFs decorated with PLGA microparticles (PCL NFs@PLGA
464 MPs), and for the PCL electrospun NFs decorated with electrosprayed thymol-loaded
465 PLGA microparticles (PCL NFs@PLGA-THY MPs), respectively. The amount of THY
466 present in the mats was also evaluated by GC-MS and similar results were obtained from

both techniques (Fig. 3E). Therefore, THY is present in the mats and is available to be released upon contact with any aqueous solution due to the hydrolytic character of its carrier (i.e., PLGA). The PLGA used has a 50:50 lactic:glycolic ratio so a sustained release over its degradation life span (< 3 months) would be expected. Drug release kinetics were evaluated in PBS with Tween 80 (2 % w/v) at 37 °C with a constant agitation (250 rpm) under sink conditions (Fig. 3F). The UPLC analysis revealed an initial burst with a 60.12 ± 7.71 wt.% of THY released in the first 3h, to be then sustained until 24h when the cumulative release measured was around 70 %.

In order to analyse the release behaviour of THY from the PLGA particles the first 60 % of the experimental release data were fitted with several mathematical models (data not shown). The Peppas-Sahlin model with a coefficient of lineal correlation (R^2) of 0.995 was chosen as the appropriate model for explaining the release kinetics [30]. The coefficient n is the purely Fickian diffusion exponent, the value of 0.69 would indicate an anomalous transport mechanism. In this kind of release mechanism, Fickian diffusion through the outer layers of the matrix and polymer chain relaxation/erosion are both involved. The constant k_1 (48.77 h^{-n}) is associated with the diffusional release while k_2 (-9.71 h^{-2n}) is related to relaxation processes. Even when the contribution of both mechanisms is considered to be additive, as the k_1/ k_2 ratio is around 5, the contribution of the Fickian diffusion would control the release process.

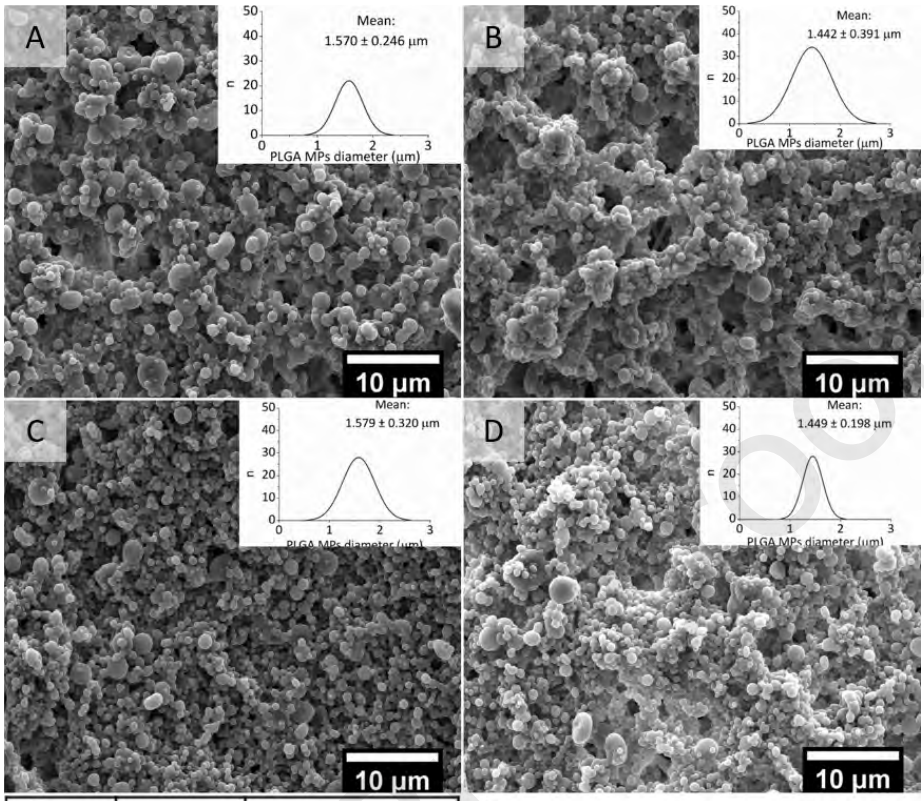

E Material	% PLGA (^{1}H-NMR, % w/w)	% THY (% w/w)	
		GC-MS	^{1}H-NMR
PCL-NFs @ PLGA MPs	11.28 ± 3.39	-	-
PCL-NFs @ PLGA-THY MPs	17.46 ± 2.15	1.30 ± 0.16	1.20 ± 0.41

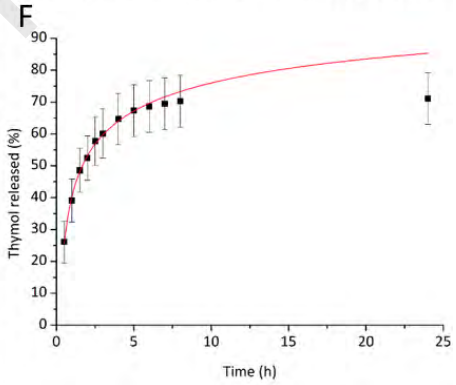

Fig. 3. Characterization of PCL NFs@PLGA-THY MPs mats: A-D) Evaluation of the attachment between the PLGA MPs and the electrospun PCL NFs by mechanical stress after 0, 6, 12 and 18 min under sonication in water, respectively; E) PLGA and THY loading in NFs evaluated by GC-MS and ^{1}H-NMR (Mean ± SD of three different samples analyzed in duplicate); F) Release profile of THY from PCL NFs@PLGA-THY MPs. Mean ± SD; 18 data per time point.

3.2. Antimicrobial and cytocompatibility of dressings

The antibacterial effect of the materials developed (PCL NFs, PCL NFs@PLGA MPs and PCL NFs@PLGA-THY MPs) against *S. aureus* was corroborated by the measurement of the inhibition zone displayed by the drug loaded electrospun disc placed on the agar as an indication of the absence of viable bacteria (Fig. 4E and F). Discs of different diameters (12, 14, 18 and 20 mm) were assayed though no antibacterial effect was found in diameters lower than 20 mm. Therefore, we set 20 mm (28.9 ± 4.6 mg) as the minimum required diameter to elicit antibacterial action considering the amount of THY loaded in the MPs attached to the electrospun mats and the bacterial burden (10^7 CFU/mL). Fig. 4 shows that, at the two time points measured (after 1 and 5 days), no inhibition zone was observed for the PCL NFs (Fig. 4A and B) or for the PCL NFs@PLGA MPs (Fig. 4C and D), but an inhibition zone around the discs was observed for the PCL NFs@PLGA-THY MPs (Fig. 4E and F), indicative of the presence of an antimicrobial compound in the medium. The diameter of the inhibition zone increased over time (24.8 ± 0.2 mm at day 1; 29.9 ± 0.6 mm after 5 days), which was indicative of a sustained release of the antimicrobial compound through the agar and that the strain used was susceptible to THY.

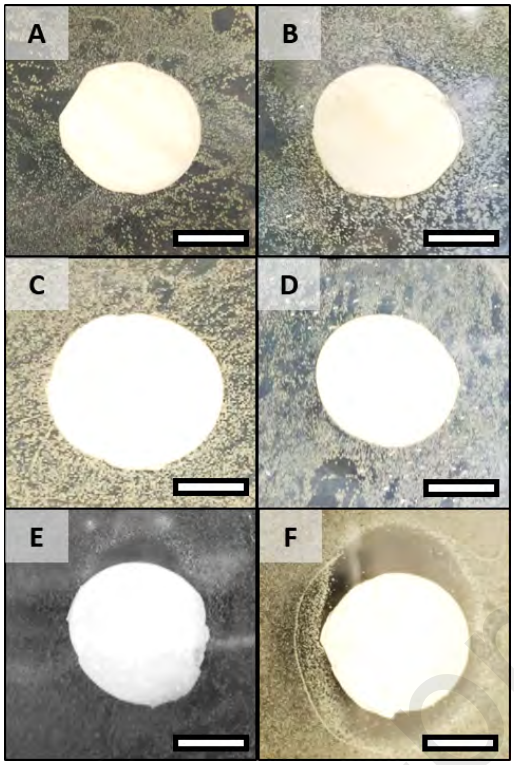

Fig. 4. Representative images of antimicrobial disk diffusion test after 1 day (A, C, E) and 5 days (B, D, F) of treatment with the different mats developed: A, B) PCL NFs; C, D) PCL NFs@PLGA MPs; E, F) PCL NFs@PLGA-THY MPs. Scale bar = 10 mm.

On the other hand, the cytocompatibility of the synthesized mats (PCL NFs, PCL NFs@PLGA MPs and PCL NFs@PLGA-THY MPs) and the corresponding free THY released in 24h (0.52 mg/mL) from the PCL NFs@PLGA-THY MPs mats (20 mm diameter) was also evaluated against human dermal fibroblasts and keratinocytes after 24h treatment. As can be seen in Fig. 5, no cytotoxicity was observed for the 20 mm mats in the time studied displaying percentages of viability above 80%. Controversially, the total amount of THY released after 24h in the mats exerted a strong cell damage with viabilities as low as 8-10% compared to the un-treated controls. According to the ISO 10993-5 standard [31], a viability above 70% is considered as the threshold for considering a

compound as non-cytotoxic and therefore, the drug loaded mats were not cytotoxic for those two cell lines studied, whereas the free monoterpenoid strongly reduced cell viability. According to the *in vitro* THY-release test (Fig. 3F) at 24h the dressings released a 71.07 ± 8.11 % of the THY loaded; hence the non-cytotoxic character of the asymmetric electrospun mats may be attributed to the sustained release of THY.

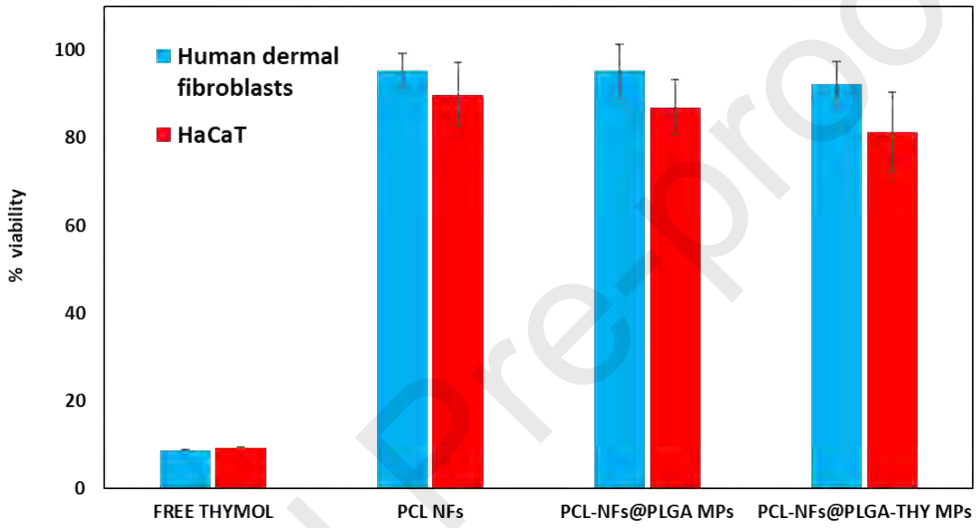

Fig. 5. *In vitro* cytotoxicity results obtained from human dermal fibroblasts and keratinocytes (HaCaT) treated for 24h with the synthesized mats (PCL NFs, PCL NFs@PLGA MPs and PCL NFs@PLGA-THY MPs) and free THY released in 24h (0.52 mg/mL) from the PCL NFs@PLGA-THY MPs mats. Mean values and SD obtained from six different experiments in duplicate (N = 12).

3.3. In vivo evaluation of the antimicrobial action of the dressings in an infection wound excisional murine model

To investigate the *in vivo* efficacy of the fabricated mats, 12-mm-diameter PCL NFs@PLGA MPs and PCL NFs@PLGA-THY MPs were evaluated in a murine excisional

wound splinting model [24], as depicted in Fig. 6A. Even though 12-mm-diameter PCL NFs@PLGA-THY MPs mats were not found to exert antibacterial effect in the inhibition zone assay, as described above, different discs of this diameter were piled up to obtain the same mats weight (28.9 ± 4.6 mg) in order to fully cover the surgical wound, achieving the same THY released as in the 20-mm-diameter disc. The use of discs of larger diameter than 12 mm was not advisable due to the wound's diameter selected in the experimental model.

Mice wound contraction was inhibited by suturing a splinting ring around the edge of the wound to mimic the human wound healing process [24]. After *S. aureus* infection, PCL NFs@PLGA MPs and PCL NFs@PLGA-THY MPs were held in place with occlusive sterile round spot adhesive plasters and sterile bandages. The control group was not treated with the fabricated mats but covered with plaster and bandages. On day 3 after surgery and infection, wounds were uncovered as recommended in the clinical practice [26,27]. Figure 6B shows that after a week, the PCL NFs@PLGA MPs and the PCL NFs@PLGA-THY MPs mats slightly reduced the bacterial load from a massive uncountable load (+++) to high bacterial counts (++). Non-treated but infected animals showed massive uncountable loads by the end of the experiment whereas not infected wounds remained uninfected until the end of the experiments (data not shown). Furthermore, microbiological qPCR (Fig. 6C) corroborated the previous findings having a significant reduction in the infective strain at 7 days post infection. 16S rRNA PCR was used to identify the specific strain *S. aureus* ATCC 25923 with a statistically significant reduction in the bacterial load quantified after 7 days of surgery and infection.

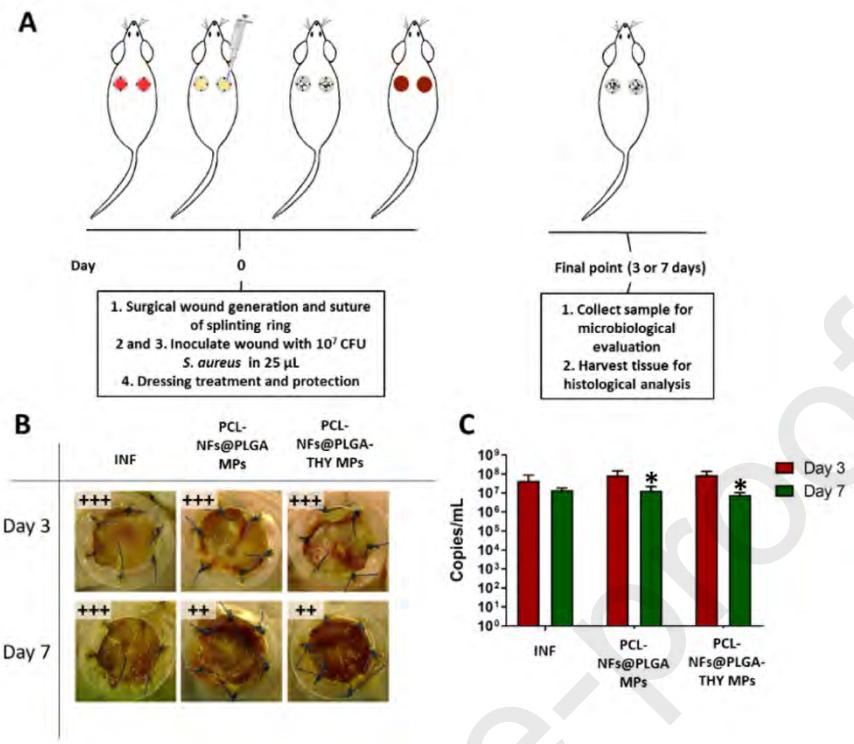

Fig. 6. *In vivo* infection wound excisional model in SKH1 mice and treatment with the synthesized materials: A) Schematic overview of the *in vivo* procedure; B) Representative images of wound evolution at 3 and 7 days after surgery and infection (INF). Insets show the microbiological results regarding bacteria colony counting ((++) high number of colonies; (+++) massive culture); C) Microbiological qPCR results. Data are expressed as Mean ± SD of three separate experiments run in triplicate. Significant differences were found between INF group vs treated groups after 7 days (*****$p \leq 0.05$).

Histopathologic studies were performed to analyze infection progress, wound repair and angiogenesis in infected and non-infected mat-treated groups (Fig. 7 and 8). Intensity of

lesions was similar in all cases between 3- and 7-days post-infection (dpi), including severe inflammation in subcutaneous tissue that reached the adipose and muscular layers of the dermis. At 7 dpi there was always a higher degree of tissue fibroplasia and repair (Fig. 7). New blood vessel formation was studied by immunostaining against CD31 and using a semi quantitative approach. Blood vessels were more abundant in the vicinity of the wound in the PCL NFs@PLGA-THY MPs treated group (Fig. 8).

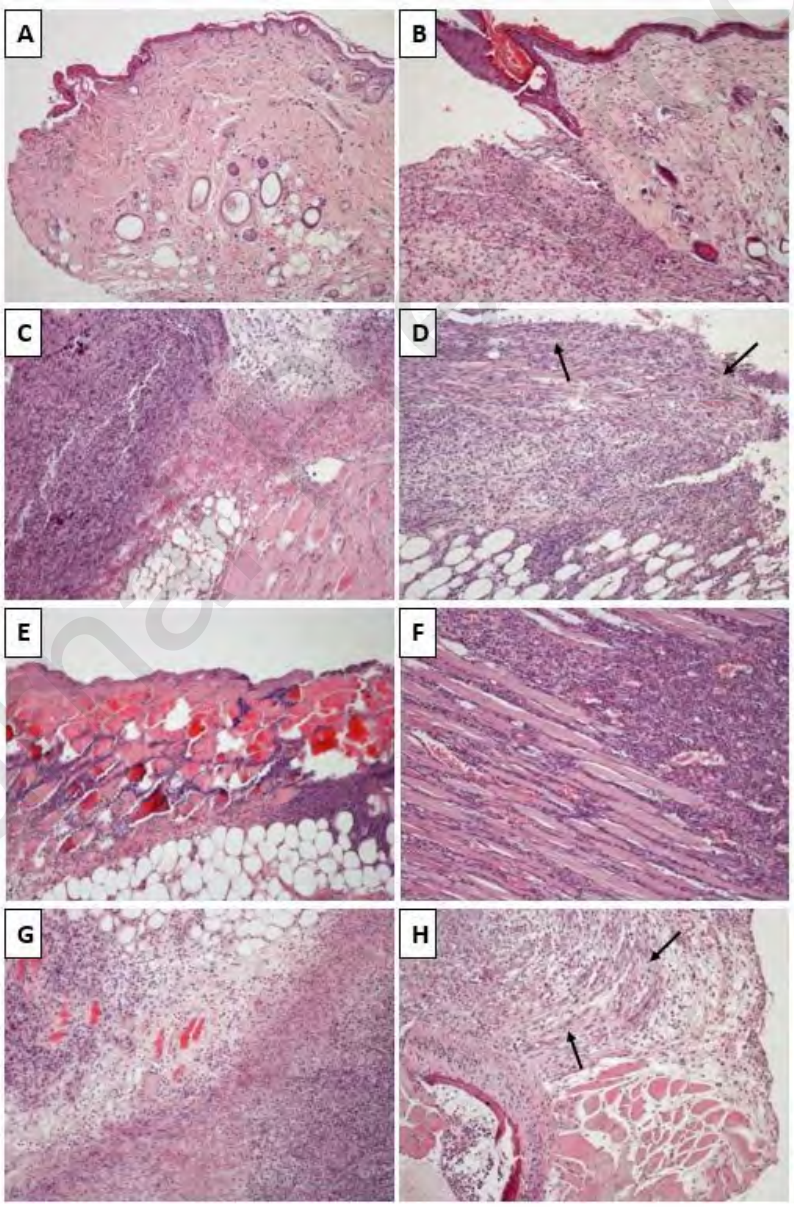

Fig. 7. Histopathological assessment of wound infection and treatment by hematoxylin-eosin staining (10x). Representative images of the control group (A, B), infection group (C, D), PCL NFs@PLGA MPs treated group (E, F) and PCL NFs@PLGA-THY MPs treated group (G, H), at 3 (A, C, E, G) and 7 (B, D, F, H) days after surgery and infection, are shown. Control animals show either no reaction around the limit of the wound (A) or formation of granulation tissue, which is characteristic of sterile wound repair (B). The infection group or both treated groups show a similar severity degree of inflammatory reaction between 3 and 7 days, compared to the controls. A higher degree of fibroplasia and repair is generally observed at 7 dpi (arrows).

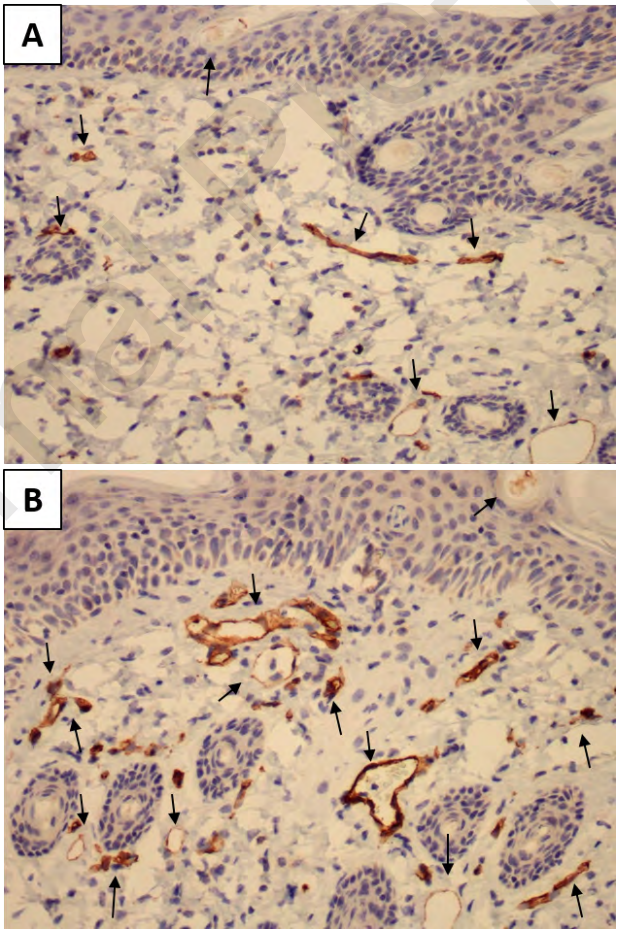

Fig. 8. Immunohistochemical staining of CD31 of the subcutaneous tissue surrounding the wound in infected and treated tissue samples at 3 dpi (20x). (A) Representative image of the infection group. Minimal presence of blood vessels (brown staining, arrows). (B) PCL NFs@PLGA-THY MPs treated group. Multiple, abundant blood vessels (brown staining, arrows).

4. Discussion

During the electrospraying process, the organic solvent present in the droplets leaving the Taylor cone rapidly evaporates, with the consequent flash polymer precipitation producing a reduced drug loss in its flight towards the counter electrode. Based on our previous experience, we decided to keep several synthesis parameters constant (needle gauge, distance to collector, solvent, temperature and humidity) and vary only two (THY concentration and flow rate). Regarding THY concentration, different THY wt.% (2.5 - 15) referred to the PLGA mass used were employed. The increase in THY concentration at the same flow rate (0.5 mL/h) did not involve significant changes in MPs sizes (Fig. 1) nor even a clear trend, as previous studies concerning PLGA MPs electrosprayed on polymeric mats have shown [32]. However, the highest THY concentration assayed (15 %) entailed an increase in MPs size up to 2.847 ± 0.706 μm though showing heterogeneous particle-size distributions. The increase in flow rate up to 1 mL/h and 10 wt.% THY concentration were found as the most appropriate conditions to obtain a homogeneous particle-size distribution (0.728 ± 0.143 μm). Interestingly, THY loaded particles did have larger size when entrapped in the fabricated mats (Fig. 2) (1.634 ± 0.277 μm). These results are in accordance with previous works that highlighted the relevance of polymeric chain entanglements in electrospraying techniques, becoming decisive in the size and

morphology of the synthesized MPs and allowing to customize the most adequate release kinetics for drug delivery purposes [32–34]. The preferential and strong attachment of PLGA MPs to PCL NFs was also demonstrated (Fig. 2 and 3), which may be related to supramolecular interactions based on the large area per volume ratio exhibited by the electrospun PCL NFs.

On the other hand, THY release kinetics were fitted into different models, being the Peppas and Sahlin model the most suitable to explain the THY release of around 60 % in the first 3h followed by a period of sustained release until 24h, reaching 70 % cumulative release (Fig. 3F). This release trend is consistent with the medium in which it was performed (PBS) and the efficient entrapment of THY in PLGA after the first hours, as previously reported [35,36]. As mentioned above, the sustained and prolonged release of antimicrobials from dressings are highly desired as infections may take place during wound healing. In addition, the use of natural substances as antimicrobial active compounds has attracted attention in the last years owing to the multiple mechanisms of antimicrobial action compared to antibiotics. In this regard, THY recommended daily dermal administration according to the European Chemicals Agency (ECHA) is below 2000 mg/kg bw [37]. Subsequently, THY release reported from our PCL NFs@PLGA-THY MPs mats is expected to be safe for wound healing applications.

Asymmetric electrospun PCL-silk fibroin and hyaluronan-silk fibroin membranes loading THY also displayed a kinetic release of THY similar to our results, showing an initial burst in the first 8h followed by a sustained release up to 24h. This trend may be connected to the high surface to volume ratio of the NFs that favors the diffusion of THY from the membranes to the release media [38].

THY biological effects are diverse, from anti-inflammatory to antibacterial. It may exert these effects at low concentrations, being different depending on the delivery system from which THY is released and on the microorganism strain challenged [35,39]. Our fabricated PCL NFs@PLGA-THY MPs mats (20 mm diameter) clearly displayed an inhibition zone in *S. aureus* inoculated agar Petri dishes (Fig. 4E and F) which increased over time (~ 5 mm at day 1, ~ 10 mm at day 5), pointing to an *in vitro* sustained release of THY. Other drug delivery systems loaded with THY have also shown the successfully inhibition of bacterial growth, such as THY enriched bacterial cellulose hydrogel (1% THY) [40], ethylcellulose/methylcellulose sub-micron spheres [39] or our previous studies regarding PCL NFs [22]. Gelatin films incorporated THY at different concentrations (1 - 8 %) also displayed antibacterial effects against *S. aureus* showing larger inhibition zones with the increase in concentration (1 - 15 mm in 24h) [41]. According to 195920-ASTM E2149-01 norm, an inhibition zone higher than 1 mm is considered as a good antibacterial agent [41]. Hence, it may be concluded that the synthesized PCL NFs@PLGA-THY MPs dressings exhibited excellent *in vitro* antibacterial properties against *S. aureus* and thus, their potential application in the clinical practice as regards infected wound treatment and healing is granted.

In this sense, the evaluation of the *in vitro* cytocompatibility of these mats in human dermal fibroblasts and keratinocytes cultures also highlighted their suitability as compatible mats (> 80 %) whereas free THY at the concentration released in 24h (0.52 mg/mL) dramatically diminished viability (8 - 10 %). This trend was also observed in previous cell viability studies involving THY loaded bacterial cellulose hydrogels in NIH 3T3 murine fibroblasts up to 72h [40] or THY loaded asymmetric electrospun PCL-silk fibroin/hyaluronan-silk

fibroin membranes in human dermal fibroblasts up to 7 days [38]. Overall, the obtained results confirm the potential of the fabricated electrospun PCL NFs@PLGA-THY MPs mats as wound dressings.

To test the *in vivo* application of the synthesized mats, we investigated their effects in an infected murine excisional wound splinting model (Fig. 6 - 8). Surgical wounds were infected with *S. aureus* ATCC 25923 and not treated (infection control group), or treated with PCL NFs@PLGA MPs or PCL NFs@PLGA-THY MPs mats. The microbiological studies (Fig. 6B and C) demonstrated the *in vivo* inhibitory potential of *S. aureus* infection showing the significant reduction of the infective strain load in treated wounds, though the total eradication of infection after treatment was not achieved due to the high bacterial load experimentally introduced (4.10^8 CFU/mL). Furthermore, only slight differences were found in wounds treated with PCL NFs@PLGA MPs or PCL NFs@PLGA-THY MPs after 7 days (10^7 copies/mL and 10^6 copies/mL, respectively). This may be related to the incomplete contact of the whole dressing with the infected wound to successfully achieve the direct exposure of bacteria with the antibacterial compound, as we previously described [22] and to the *in vivo* diffusion and washing of the antimicrobial compound. It should be noted that different discs of the mats of 12 mm of diameter were piled up to cover the infected wounds in order to obtain the same mats mass and amounts of THY released as the one displayed by the membranes used in the *in vitro* assays regarding the inhibition of bacteria growth. Thus, only the disc in direct contact with the wound may exert the antimicrobial action but not those which were above, hampering the potential inhibitory effects of released THY on bacterial growth. Moreover, previous studies have highlighted that the amount of drug or natural compound released from loaded scaffolds in PBS may

not be the same as that released on an agar plate arising from the differences in drug or natural compound solubility and/or solution volume, though the relative trends may be similar since PBS and agar has the same pH [36]. Taking this observation into account, the environment present in a wound may play a key role in drug or natural compound released and thus, in its biological effects, regarding the presence of different substances (i.e. cytokines, vitamins, hormones, enzymes) whose levels dynamically change in the different stages of healing [42]. Therefore, it is expected that the release trend of a compound may differ in *in vitro* and *in vivo* conditions as we describe, being not feasible to exactly mimic *in vitro* the *in vivo* microenvironment of an infected wound due to its complexity and multistage dynamic nature.

5. Conclusions

This study presents the development of electrospun PCL-based mats incorporating PLGA MPs loading THY as antibacterial compound. Dressings with a THY load higher than 1.2 % w/w were achieved. The fabricated mats were able to successfully inhibit *S. aureus in vitro* growth when containing THY. Their cytocompatibility was also demonstrated showing viabilities higher than 80 % in human dermal fibroblasts and keratinocytes cultures after 24h treatment, whereas free THY at the same concentration released after 24h was significantly detrimental for eukaryotic cells. *In vivo* studies involved the development of the murine excisional wound splinting model followed by the infection of wounds with a high load of *S. aureus* and their treatment with the synthesized dressings. The microbiological and histopathological evaluation of the wounds after 3 and 7 days of surgery and infection revealed the inhibition of the bacteria load in wounds after 7 days though the complete eradication of the infection was not obtained. Moreover, PCL

NFs@PLGA MPs and PCL NFs@PLGA-THY MPs dressings displayed similar results, which may be related with the circumscribed inhibitory effect of the THY loaded dressings to the contact area with the wound, as we previously described, and the differences in THY release *in vitro* and *in vivo*. This work validates *in vivo* our previous observations regarding the importance of the close contact between the antibacterial dressing and pathogenic bacteria, highlighting the need to customize or adapt the dressing considering the wound surface and the antimicrobial compound loading.

Acknowledgements

This research was funded by the Spanish Ministry of Economy and Competitiveness (grant number CTQ2014-52384-R). Financial support from the EU thanks to the ERC Consolidator Grant program (ERC-2013-CoG-614715, NANOHEDONISM) is also acknowledged. CIBER-BBN is an initiative funded by the VI National R&D&i Plan 2008 - 2011, Iniciativa Ingenio 2010, Consolider Program, CIBER Actions and financed by the Instituto de Salud Carlos III (Spain) with assistance from the European Regional Development Fund. We acknowledge the Histopathology Unit from CNIO, LMA-INA and Cell Culture, Animal Care and Pathological Anatomy Core Units from IACS/IIS Aragon for their instruments and expertise. The authors are grateful to Dr Elena Tapia, Dr Montserrat Perez-Piñero, Dr Ander Izeta, and Dr Laura Yndriago for helpful advice and comments regarding the *in vivo* wound model. S.G-S. and M.S-A also acknowledge the support from the FPI and FPU programs, respectively, both fellowships granted by the Spanish Ministry of Science, Innovation and Universities. G.M. gratefully acknowledges the support from the Miguel Servet Program (MS19/00092; Instituto de Salud Carlos III).

Declaration of Competing Interest

No potential conflicts of interest were disclosed.

References

[1] S.R. Nussbaum, M.J. Carter, C.E. Fife, J. DaVanzo, R. Haught, M. Nusgart, D. Cartwright, An Economic Evaluation of the Impact, Cost, and Medicare Policy Implications of Chronic Nonhealing Wounds, Value Heal. 21 (2018) 27–32. https://doi.org/10.1016/J.JVAL.2017.07.007.

[2] M. Olsson, K. Järbrink, U. Divakar, R. Bajpai, Z. Upton, A. Schmidtchen, J. Car, The humanistic and economic burden of chronic wounds: A systematic review, Wound Repair Regen. 27 (2019) 114–125. https://doi.org/10.1111/wrr.12683.

[3] E. Sanchez-Rexach, E. Meaurio, J.-R. Sarasua, Recent developments in drug eluting devices with tailored interfacial properties, Adv. Colloid Interface Sci. 249 (2017) 181–191. https://doi.org/10.1016/J.CIS.2017.05.005.

[4] S. Silver, Bacterial silver resistance: molecular biology and uses and misuses of silver compounds, FEMS Microbiol. Rev. 27 (2003) 341–353. https://doi.org/10.1016/S0168-6445(03)00047-0.

[5] N. Tanaka, Biochemical studies on gentamicin resistance., J. Antibiot. (Tokyo). 23 (1970) 469–71.

[6] B. Seitz, S. Hayashi, W.R. Wee, L. LaBree, P.J. McDonnell, In vitro effects of aminoglycosides and fluoroquinolones on keratocytes., Invest. Ophthalmol. Vis. Sci. 37 (1996) 656–65.

[7] D.W. Chen, Y.-H. Hsu, J.-Y. Liao, S.-J. Liu, J.-K. Chen, S.W.-N. Ueng, Sustainable release of vancomycin, gentamicin and lidocaine from novel electrospun sandwich-structured PLGA/collagen nanofibrous membranes, Int. J. Pharm. 430 (2012) 335–341. https://doi.org/10.1016/J.IJPHARM.2012.04.010.

[8] A. Burd, C.H. Kwok, S.C. Hung, H.S. Chan, H. Gu, W.K. Lam, L. Huang, A comparative study of the cytotoxicity of silver-based dressings in monolayer cell, tissue explant, and animal models, Wound Repair Regen. 15 (2007) 94–104. https://doi.org/10.1111/j.1524-475X.2006.00190.x.

[9] J.J. Elsner, I. Berdicevsky, M. Zilberman, In vitro microbial inhibition and cellular response to novel biodegradable composite wound dressings with controlled release of antibiotics, Acta Biomater. 7 (2011) 325–336. https://doi.org/10.1016/j.actbio.2010.07.013.

[10] C. Kimna, S. Tamburaci, F. Tihminlioglu, Novel zein-based multilayer wound dressing membranes with controlled release of gentamicin, J. Biomed. Mater. Res. - Part B Appl. Biomater. (2018). https://doi.org/10.1002/jbm.b.34298.

[11] W.K.W. Abdul Khodir, A.H. Abdul Razak, M.H. Ng, V. Guarino, D. Susanti, Encapsulation and Characterization of Gentamicin Sulfate in the Collagen Added Electrospun Nanofibers for Skin Regeneration., J. Funct. Biomater. 9 (2018). https://doi.org/10.3390/jfb9020036.

[12] D. Egozi, M. Baranes-Zeevi, Y. Ullmann, A. Gilhar, A. Keren, E. Matanes, I. Berdicevsky, N. Krivoy, M. Zilberman, M. Zilberman, Biodegradable soy wound dressings with controlled release of antibiotics: Results from a guinea pig burn

model, (2015). https://doi.org/10.1016/j.burns.2015.03.013.

[13] L. Wu, G. Norman, J.C. Dumville, S. O'Meara, S.E. Bell-Syer, Dressings for treating foot ulcers in people with diabetes: an overview of systematic reviews, Cochrane Database Syst. Rev. (2015). https://doi.org/10.1002/14651858.CD010471.pub2.

[14] K. Twum-Danso, C. Grant, S.A. Al-Suleiman, S. Abdel-Khader, M.S. Al-Awami, H. Al-Breiki, S. Taha, A.-A. Ashoor, L. Wosornu, Microbiology of postoperative wound infection: a prospective study of 1770 wounds, J. Hosp. Infect. 21 (1992) 29–37. https://doi.org/10.1016/0195-6701(92)90151-B.

[15] A. Rastogi, S. Sukumar, A. Hajela, S. Mukherjee, P. Dutta, S.K. Bhadada, A. Bhansali, The microbiology of diabetic foot infections in patients recently treated with antibiotic therapy: A prospective study from India, J. Diabetes Complications. 31 (2017) 407–412. https://doi.org/10.1016/J.JDIACOMP.2016.11.001.

[16] Y.-K. Wu, N.-C. Cheng, C.-M. Cheng, Biofilms in Chronic Wounds: Pathogenesis and Diagnosis, Trends Biotechnol. 37 (2019) 505–517. https://doi.org/10.1016/J.TIBTECH.2018.10.011.

[17] G. Schultz, T. Bjarnsholt, G.A. James, D.J. Leaper, A.J. McBain, M. Malone, P. Stoodley, T. Swanson, M. Tachi, R.D. Wolcott, Global Wound Biofilm Expert Panel, Consensus guidelines for the identification and treatment of biofilms in chronic nonhealing wounds, Wound Repair Regen. 25 (2017) 744–757. https://doi.org/10.1111/wrr.12590.

[18] M. Michalska-Sionkowska, M. Walczak, A. Sionkowska, Antimicrobial activity of

collagen material with thymol addition for potential application as wound dressing, Polym. Test. 63 (2017) 360–366. https://doi.org/10.1016/j.polymertesting.2017.08.036.

[19] S. García-Salinas, H. Elizondo-Castillo, M. Arruebo, G. Mendoza, S. Irusta, Evaluation of the Antimicrobial Activity and Cytotoxicity of Different Components of Natural Origin Present in Essential Oils, Molecules. 23 (2018) 1399. https://doi.org/10.3390/molecules23061399.

[20] R.J.W. Lambert, P.N. Skandamis, P.J. Coote, G.-J.E. Nychas, A study of the minimum inhibitory concentration and mode of action of oregano essential oil, thymol and carvacrol, J. Appl. Microbiol. 91 (2001) 453–462. https://doi.org/10.1046/j.1365-2672.2001.01428.x.

[21] K.R. Riella, R.R. Marinho, J.S. Santos, R.N. Pereira-Filho, J.C. Cardoso, R.L.C. Albuquerque-Junior, S.M. Thomazzi, Anti-inflammatory and cicatrizing activities of thymol, a monoterpene of the essential oil from Lippia gracilis, in rodents, J. Ethnopharmacol. 143 (2012) 656–663. https://doi.org/10.1016/J.JEP.2012.07.028.

[22] E. Gámez, G. Mendoza, S. Salido, M. Arruebo, S. Irusta, Antimicrobial Electrospun Polycaprolactone-Based Wound Dressings: An In Vitro Study About the Importance of the Direct Contact to Elicit Bactericidal Activity , Adv. Wound Care. (2019). https://doi.org/10.1089/wound.2018.0893.

[23] A.W. Bauer, W.M.M. Kirby, J.C. Sherris, M. Turck, Antibiotic Susceptibility Testing by a Standardized Single Disk Method, Am. J. Clin. Pathol. 45 (1966) 493–496. https://doi.org/10.1093/ajcp/45.4_ts.493.

[24] X. Wang, J. Ge, E.E. Tredget, Y. Wu, The mouse excisional wound splinting model, including applications for stem cell transplantation, Nat. Protoc. 8 (2013) 302–309. https://doi.org/10.1038/nprot.2013.002.

[25] R.D. Galiano, J. Michaels, V, M. Dobryansky, J.P. Levine, G.C. Gurtner, Quantitative and reproducible murine model of excisional wound healing, Wound Repair Regen. 12 (2004) 485–492. https://doi.org/10.1111/j.1067-1927.2004.12404.x.

[26] Dressings - Clinical guidelines, (n.d.). https://medicalguidelines.msf.org/viewport/CG/english/dressings-18482377.html#id-.DressingsvEnglish-Removalofanolddressing (accessed September 7, 2019).

[27] NICE Clinical Guidelines, Appendix C. Wound dressings for surgical site infection prevention, in: L.R. Press (Ed.), Surg. Site Infect. Prev. Treat. Surg. Site Infect., 2008.

[28] J. Aragón, S. Feoli, S. Irusta, G. Mendoza, Composite scaffold obtained by electro-hydrodynamic technique for infection prevention and treatment in bone repair, Int. J. Pharm. 557 (2019) 162–169. https://doi.org/10.1016/j.ijpharm.2018.12.002.

[29] R.B. Trinca, C.B. Westin, J.A.F. da Silva, Â.M. Moraes, Electrospun multilayer chitosan scaffolds as potential wound dressings for skin lesions, Eur. Polym. J. 88 (2017) 161–170. https://doi.org/10.1016/J.EURPOLYMJ.2017.01.021.

[30] N.A. Peppas, J.J. Sahlin, A simple equation for the description of solute release. III. Coupling of diffusion and relaxation, Int. J. Pharm. 57 (1989) 169–172. https://doi.org/10.1016/0378-5173(89)90306-2.

[31] ISO 10993-5:2009 - Biological evaluation of medical devices -- Part 5: Tests for in vitro cytotoxicity, (n.d.). https://www.iso.org/standard/36406.html (accessed June 4, 2019).

[32] L. Mayol, A. Borzacchiello, V. Guarino, C. Serri, M. Biondi, L. Ambrosio, Design of electrospayed non-spherical poly (L-lactide-co-glicolide) microdevices for sustained drug delivery., J. Mater. Sci. Mater. Med. 25 (2014) 383–90. https://doi.org/10.1007/s10856-013-5080-5.

[33] V. Guarino, V. Cirillo, P. Taddei, M.A. Alvarez-Perez, L. Ambrosio, Tuning size scale and crystallinity of PCL electrospun fibres via solvent permittivity to address hMSC response., Macromol. Biosci. 11 (2011) 1694–705. https://doi.org/10.1002/mabi.201100204.

[34] Y. Wu, R.L. Clark, Electrohydrodynamic atomization: a versatile process for preparing materials for biomedical applications., J. Biomater. Sci. Polym. Ed. 19 (2008) 573–601. https://doi.org/10.1163/156856208784089616.

[35] S. Milovanovic, D. Markovic, A. Mrakovic, R. Kuska, I. Zizovic, S. Frerich, J. Ivanovic, Supercritical CO2 - assisted production of PLA and PLGA foams for controlled thymol release, Mater. Sci. Eng. C. 99 (2019) 394–404. https://doi.org/10.1016/J.MSEC.2019.01.106.

[36] E. Buck, V. Maisuria, N. Tufenkji, M. Cerruti, Antibacterial Properties of PLGA Electrospun Scaffolds Containing Ciprofloxacin Incorporated by Blending or Physisorption, ACS Appl. Bio Mater. 1 (2018) 627–635. https://doi.org/10.1021/acsabm.8b00112.

[37] Thymol - Registration Dossier - ECHA, (n.d.). https://euon.echa.europa.eu/lt/web/guest/registration-dossier/-/registered-dossier/11030/7/3/4 (accessed August 23, 2019).

[38] S.P. Miguel, D. Simões, A.F. Moreira, R.S. Sequeira, I.J. Correia, Production and characterization of electrospun silk fibroin based asymmetric membranes for wound dressing applications., Int. J. Biol. Macromol. 121 (2019) 524–535. https://doi.org/10.1016/j.ijbiomac.2018.10.041.

[39] A. Wattanasatcha, S. Rengpipat, S. Wanichwecharungruang, Thymol nanospheres as an effective anti-bacterial agent, Int. J. Pharm. 434 (2012) 360–365. https://doi.org/10.1016/J.IJPHARM.2012.06.017.

[40] S. Jiji, S. Udhayakumar, C. Rose, C. Muralidharan, K. Kadirvelu, Thymol enriched bacterial cellulose hydrogel as effective material for third degree burn wound repair., Int. J. Biol. Macromol. 122 (2019) 452–460. https://doi.org/10.1016/j.ijbiomac.2018.10.192.

[41] G. Kavoosi, S.M.M. Dadfar, A.M. Purfard, Mechanical, physical, antioxidant, and antimicrobial properties of gelatin films incorporated with thymol for potential use as nano wound dressing., J. Food Sci. 78 (2013) E244-50. https://doi.org/10.1111/1750-3841.12015.

[42] O. Castaño, S. Pérez-Amodio, C. Navarro-Requena, M.Á. Mateos-Timoneda, E. Engel, Instructive microenvironments in skin wound healing: Biomaterials as signal releasing platforms, Adv. Drug Deliv. Rev. 129 (2018) 95–117. https://doi.org/10.1016/j.addr.2018.03.012.

946